Non-linear vibration analysis of visco-elastically damped composite structures by multilevel finite elements and asymptotic numerical method

Guillaume Robin, El Mostafa Daya, Hakim Boudaoud, Elias Belouettar-Mathis, Ahmed Makradi, Salim Belouettar

Composites Part C: Open Access 7 (2022) 100240

Contents lists available at ScienceDirect

Composites Part C: Open Access

journal homepage: www.elsevier.com/locate/composites-part-c-open-access

Non-linear vibration analysis of visco-elastically damped composite structures by multilevel finite elements and asymptotic numerical method

Guillaume Robin [a], El Mostafa Daya [a], Hakim Boudaoud [b], Elias Belouettar-Mathis [d], Ahmed Makradi [c], Salim Belouettar [c,*]

[a] Université de Lorraine, LEM3, LabEx DAMAS, F-57000 METZ, France
[b] Université de Lorraine, Equipe de Recherche des Processus Innovatifs, EA-3767, F-54000 NANCY, France
[c] Luxembourg Institute of Science and Technology, Luxembourg
[d] Centrale Marseille, 38 Rue Frédéric Joliot Curie, 13013 Marseille, France

ARTICLE INFO

Keywords:
Vibrations
Damping
Multiscale finite element method (FE^2)
Asymptotic Numerical Method
Nonlinear homogenization
Automatic differentiation

ABSTRACT

Composite materials and structures are inherently in-homogeneous across multiple scales. Multi-scale modelling offers opportunities to apprehend the coupling of material behaviour and characteristics from the micro- to meso- and macro-scales. In this paper, a multi-scale finite element method (FE^2) is proposed to compute the modal properties of visco-elastic heterogeneous composite materials in terms of damping frequencies and modal loss factors. In the proposed FE^2-based vibration analysis, two finite elements (FE) calculations are carried out in a nested manner, one at the macro-scale and the other at the micro-scale. Unlike conventional analysis, the developed analysis does not require homogenized constitutive properties because these are derived from the micro-scale FE simulations at the representative volume element (RVE) level. The non-linearity at the micro-scale is accounted by using a frequency dependent Young's modulus. The Asymptotic Numerical Method (ANM) and its automatic differentiation is used to solve the non-linear numerical problem. ANM consists of solving an analytical non-linear problem with a path-following (or continuation) method associated with a high-order perturbation technique. Compared with existing methods, the originality of the proposed approach lies in its ability to account for the frequency dependence of Young's modulus in visco-elastic microstructure. Using the automatic differentiation makes the proposed approach enough flexible and generic to deal with damped and undamped vibration analyses of composite materials structures.

1. Introduction

The estimation of the structural damping properties (modal frequencies and loss factors) of composite materials and structures has been an important subject of research and technological questions over the last decades and remarkably high numbers of papers have been published on the subject. The review by Mastroddi et al. [1] on time and frequency domain linear visco-elastic modelling of highly damped structures and the review by Chaudhary et al. [2] on the vibration damping materials and their applications should be reported. Despite the efforts and the important contributions of many research groups including research works of the authors [3–8], this field has been like crystallized around some very limiting models and design rules using a general linear visco-elastic formulation [9–11]. These models are too restrictive to obtain effective technical solutions, especially when large frequency regime and microstructure–structure coupling are considered [8,9,12–17]. Therefore, the research challenges is to propose efficient numerical methods to solve these non-linear problems in order to determine the damping properties.

In vibration analysis, the frequency dependence of material properties leads to non-linear eigenvalue problems that cannot be solved by conventional numerical methods [3]. The damping properties can be obtained only if the design process effectively integrates the micro-structural response and morphology. Nevertheless, this very important aspect of "material by design" has not been fully exploited yet. In fact, if composite micro-structure design is decisive in the realization of modern vibration damping, it is a matter of fact that, at present, this micro-structure design is usually done following some known empirical rules that do not allow for a true optimization of their dynamical performances.

A series of micro-mechanical approaches for the estimation of the damping properties of composite material as a function of the properties of the constituent materials has been developed in [8,18–20].

* Corresponding author.
E-mail address: salim.belouettar@list.lu (S. Belouettar).

https://doi.org/10.1016/j.jcomc.2022.100240
Received 9 December 2021; Received in revised form 3 February 2022; Accepted 6 February 2022
Available online 19 February 2022

Recent works proposed to use finite element (FE) solutions in multi-scale context where the macroscopic parameters are obtained by volume averaging over statistically representative volume, which are then used at the macroscopic level [20,21]. These approaches are based on a hierarchical decomposition of the solution space into a local solution and a global one and by enforcement of the compatibility conditions. This multilevel finite element methodology is introduced where the hierarchical character of model descriptions and simulation results are exploited to expedite the analysis of the problem. This approach could provide significant insights in the prediction of dynamical properties of heterogeneous and visco-elastically reinforced composites, which makes it ideal for micro/macro analyses where solutions from a local model are used to derive the solution of the macroscopic model. For instance, in [20], a multi-scale approach consisting of two scales transition models has been proposed for the analysis of heterogeneous micro-structure RVE. An energy-based finite element method is proposed in order to determine the tangent modulus of the RVE and a classical analytical micro-mechanical model is used at the second scale to determine the effective stiffness and loss tensors.

FE^2 [22] is an increasingly popular class of multiscale methods because of its versatility to model heterogeneous material behaviour across multiple scales. In classical FE^2 analysis, two finite elements calculations are carried out in a nested manner, one at the macro-scale and the other at the micro-scale. Unlike conventional analyses, the macro-scale FE analysis does not require homogenized constitutive properties because these are derived from FE simulations at the RVE level [20,23,24]. In the framework of the FE^2 method, the vibration issue is formulated at two scales: the macroscopic scale that represents the whole structure to be studied and the microscopic scale represented by the RVE. Notice that the efficiency of the method depends on the choice of the RVE and that the classical FE^2 method is still heavy when dealing with high non-linearity problems or 3D real structures [25]. To overcome this shortcoming, a data-driven method based on FE^2 is proposed in [26] to substitute the heavy micro-level FE simulations [27].

This work aims to develop an FE^2 multi-level materials modelling and design approach for the vibration modelling and analysis of heterogeneous composite materials that accounts for material micro-structure non-linearity. The Asymptotic Numerical Method (ANM) [28,29] is used to solve the non-linear problem at the macro-scale. The integrated model is employed to observe the influence of micro-structure heterogeneity on the natural frequencies and modal loss factors of a composite structure. The paper is organized into five sections. In Section 2, the multi-scale formulation of the vibration problem is presented. The solution strategy of the multi-scale problem is elaborated in Section 3. Section 4 is devoted to numerical tests to assess and validate the proposed methodology. In Section 5, the approach is used to design visco-elastic sandwich beams with optimized damping properties. Finally, Section 6 presents some conclusions.

2. Multi-scale formulation of the vibration problem

2.1. Macroscopic problem formulation

We consider a composite structure characterized by a periodic micro-structure as depicted in Fig. 2. In the framework of a multilevel FE^2 approach, the macro-scale structure is considered as homogeneous and represented by the domain Φ in $\mathbb{R}^D$ (D being the domain dimension) with external boundary $\partial\Phi$ as shown in Fig. 2. The structure is subjected to prescribed displacements and forces on the disjoint complementary parts of the boundary $\partial\Phi_{\overline{u}}$ (Dirichlet boundaries) and $\partial\Phi_{\overline{T}}$ (Neumann boundary), respectively, such that $\partial\Phi_{\overline{u}} \cap \partial\Phi_{\overline{T}} = \emptyset$ and $\partial\Phi_{\overline{u}} \cup \partial\Phi_{\overline{T}} = \partial\Phi$.

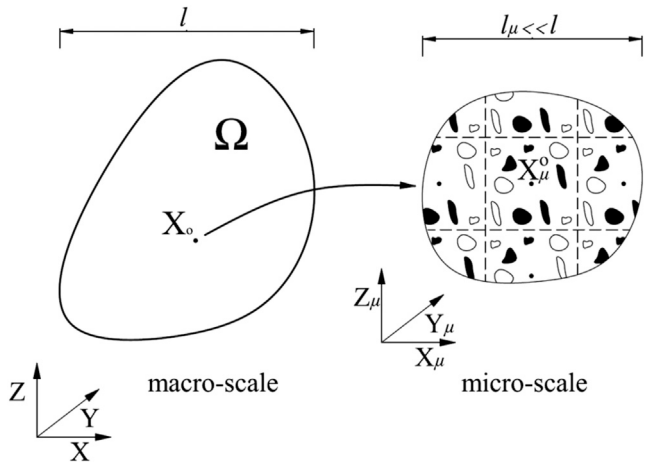

Fig. 1. Schematic representation of the heterogeneous composite structure with periodic microstructure [30].

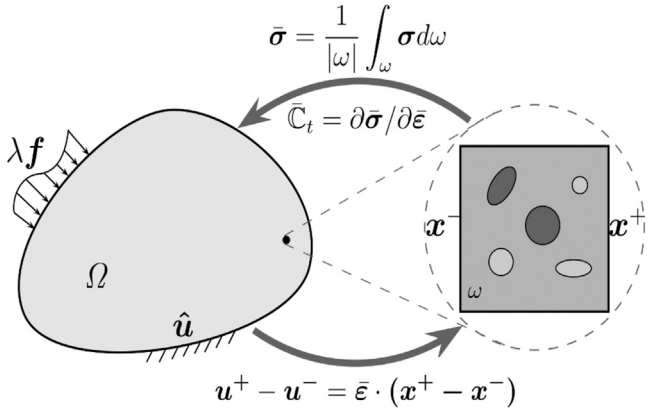

Fig. 2. Representation of the Multi-level Modelling Approach based on the FE^2 Method. The exponents + and − are associated with nodal indices on opposite sides of the RVE with microscopic boundary conditions depending on the macroscopic strain tensor. ω is the volume of the RVE.

In the context of infinitesimal strain theory and in the absence of body forces, the free vibration problem to be solved is defined as follows:

$$\begin{cases} \nabla \cdot \overline{\sigma} = \overline{\rho}\dfrac{\partial^2 \overline{u}}{\partial t^2} & \forall\ \overline{X} \in \Phi \\ \overline{u}\left(\overline{X}\right) = \hat{u}\left(\overline{X}\right) & \forall\ \overline{X} \in \partial\Phi_{\overline{u}} \\ \overline{\sigma} \cdot \overline{n} = \overline{T} & \forall\ \overline{X} \in \partial\Phi_{\overline{T}} \\ \overline{\varepsilon} = \dfrac{1}{2}\left(\nabla\overline{u} +^T \nabla\overline{u}\right) & \end{cases} \tag{1}$$

An overline is used to denote macroscopic quantities: $\overline{\sigma}$ is the macroscopic Cauchy stress tensor, $\overline{\varepsilon}$ is the macroscopic strain tensor and $\overline{\rho}$ indicates the material density. The term $\overline{u}$ denotes the macroscopic displacement field whereas $\hat{u}$ are the prescribed displacement, $\overline{X}$ is the coordinate of a given point in the structure. $\overline{n}$ is the outward unit normal vector to $\partial\Phi$. The principle of the virtual work gives the weak form of the free vibration problem associated with Eq. (1) as:

$$\int_\Phi \overline{\sigma} : \delta\overline{\varepsilon}\, d\Phi + \int_\Phi \overline{\rho}\frac{\partial^2 \overline{u}}{\partial t^2}\delta\overline{u}\, d\Phi = 0 \tag{2}$$

The constitutive relationship between $\overline{\sigma}$ and $\overline{\varepsilon}$ is given by Hooke's law:

$$\overline{\sigma} = \overline{C} : \overline{\varepsilon} \tag{3}$$

where $\overline{C}$ is a fourth-order tensor of the behaviour of the macroscopic structure. At this stage, this tensor is assumed to be unknown and can be estimated in a multi-scale analysis by solving a local finite element problem at the micro-structure level, see Fig. 2.

2.2. Formulation of the micro-scale problem

The analysed micro-structure is heterogeneous as shown in Fig. 1. This micro-structure is characterized by an RVE that occupies a domain ϕ in $\mathbb{R}^D$ with external boundary $\partial\phi$. In the absence of body forces and inertia effects, the equilibrium equations are given by the following relation:

$$\nabla \cdot \sigma = 0 \quad \forall\ X \in \phi \tag{4}$$

where σ is the microscopic Cauchy stress tensor. Note that the inertia effects are neglected at the microscopic level, as in [31–33], in order to allow for a numerical micro-to-macro transition. This hypothesis is valid as the micro-structure size is smaller than the wavelength and the analysis applies for low and medium frequency ranges.

The associated weak form of the microscopic problem is written as:

$$\int_{\phi} \sigma : \delta\varepsilon \, d\phi = 0 \tag{5}$$

where ε denotes the strain tensor at the microscopic scale defined as:

$$\varepsilon = \frac{1}{2}\left(\nabla u + {}^{T}\nabla u\right) \tag{6}$$

The constitutive relationship between σ and ε is given as:

$$\sigma = C^{(r)} : \varepsilon \tag{7}$$

where $C^{(r)}$ is the fourth order constitutive tensor associated with the phase (r). At this stage, this tensor is known for each phase (r).

2.3. Micro- & macro-scales coupling

The macroscopic stress tensor $(\overline{\sigma})$ can be computed from the microscopic tensor through three main coupling relations. The first relation expresses the macroscopic stress tensor $(\overline{\sigma})$ as the average value of the microscopic one (σ) [34]:

$$\overline{\sigma} = \langle\sigma\rangle = \frac{1}{|\,\phi\,|}\int_{\phi} \sigma \, d\phi \tag{8}$$

where $|\ \phi\ |$ represents the volume of the RVE. The second relation expresses the macroscopic strain tensor $(\overline{\varepsilon})$ as the average value of the microscopic one (ε):

$$\overline{\varepsilon} = \langle\varepsilon\rangle = \frac{1}{|\,\phi\,|}\int_{\phi} \varepsilon \, d\phi \tag{9}$$

The last formula is the energy average theorem of Hill–Mandel [34]:

$$\overline{\sigma} : \delta\overline{\varepsilon} = \langle\sigma : \delta\varepsilon\rangle = \frac{1}{|\,\phi\,|}\int_{\phi} \sigma : \varepsilon \, d\phi \tag{10}$$

2.4. Microscopic boundary conditions

Different types of microscopic boundary conditions such as linear deformation, uniform traction, or periodic constraints can be selected [35]. The following periodic conditions, on the boundary of the RVE, are considered:

$$u^{+} - u^{-} = \overline{\varepsilon} \cdot \left(X^{+} - X^{-}\right) \quad \forall\ X \in \partial\phi \tag{11}$$

It should be noted that the behaviour of a visco-elastic material may depend on its vibration frequency. The fourth-order constitutive tensor $C^{(r)}$, associated with visco-elastic phases of the material at the micro-scale, can be written as follows:

$$C^{v} = E^{*}(0)C_0 + E(\lambda)C_0 \tag{12}$$

where $E^{*}(0)$ is related to the delayed elasticity [36], $E(\lambda)$ is a function that introduces the frequency dependence, λ is the eigenvalue of the structure and ν is the Poisson ratio. We consider $\lambda = \omega^2$ where ω is the circular vibration frequency. C_0 is defined as follows:

$$C_0 = \frac{1}{1-\nu^2}\begin{bmatrix} 1 & \nu & 0 \\ \nu & 1 & 0 \\ 0 & 0 & \dfrac{1-\nu}{2} \end{bmatrix} \tag{13}$$

Introducing Eq. (12) into Eq. (5) and (7), the microscopic problem to be solved can be written as follow:

$$\begin{cases} \displaystyle\int_{\phi_e} {}^{T}\nabla u : C_e : \nabla\delta u \, d\phi_e + E^{*}(0)\int_{\phi_v} {}^{T}\nabla u : C_0 : \nabla\delta u \, d\phi_v + \\ \displaystyle E(\lambda)\int_{\phi_v} {}^{T}\nabla u : C_0 : \nabla\delta u \, d\phi_v = 0 \\ u^{+} - u^{-} = \overline{\varepsilon} \cdot \left(X^{+} - X^{-}\right) \quad \forall\ X \in \partial\phi \end{cases} \tag{14}$$

where ϕ_e and ϕ_v are, respectively, the domains occupied by the elastic and visco-elastic materials in the RVE. The obtained problem is non-linear with a material viscoelastic behaviour considered as frequency dependent. The detailed problem solving strategy is presented in the next section.

3. Multiscale solution strategy

The strategy to solve the multi-scale problem is herein presented. Considering the coupling conditions between macroscopic and microscopic problems, the microscopic problem is first solved. Then, the obtained solution is used to construct numerically the localization tensors [37] and then to map the obtained solution in order to estimate the macroscopic tangent modulus. Classically, the localization tensor is constructed by using the superposition principle, which is valid only for linear problems. Since the microscopic problem (14) is nonlinear, ANM is used to construct a sequence of linear problems such that the superposition principle can be applied. Details about the ANM can be found in [38,39].

3.1. Linearization of the microscopic problem using ANM

ANM uses a perturbation technique where the unknowns $(u,\ \lambda)$ of the problem (14) are expanded into power series with respect to a path parameter a that will be defined later. In the analysed case, the function $E(\lambda)$, which represents the frequency dependence, is expanded into power series, as follows:

$$\begin{cases} u(a) = u_0 + \displaystyle\sum_{i=1}^{N} a^i u_i \\ \lambda(a) = \lambda_0 + \displaystyle\sum_{i=1}^{N} a^i \lambda_i \\ E(a) = E_0 + \displaystyle\sum_{i=1}^{N} a^i E_i \end{cases} \tag{15}$$

$(u_0,\ \lambda_0)$ is the solution of multi-scale problem formulated at the microstructure level by considering only the real part of Young's modulus in the viscoelastic phase. Introducing the power series development (Eq. (15)) into problem in Eq. (14) and equating the same powers of a, the following set of linear problems is obtained:

Order 1.

$$\begin{cases} \mathcal{L}(u_1, \delta u) = -E_1 \displaystyle\int_{\phi_v} {}^{T}\nabla u_0 : C_0 : \nabla\delta u \, d\phi_v & \forall X \in \phi \\ u_1^{+} - u_1^{-} = \overline{\varepsilon} \cdot (X^{+} - X^{-}) & \forall X \in \partial\phi \end{cases} \tag{16}$$

Order $k \geq 2$.

$$\begin{cases} \mathcal{L}(u_k, \delta u) = -\sum_{m=0}^{k-1} E_{k-m} \int_{\phi_v} {}^T\nabla u_m : C_0 : \nabla \delta u \, d\phi_v & \forall X \in \phi \\ u_k^+ - u_k^- = \overline{\varepsilon} \cdot (X^+ - X^-) & \forall X \in \partial\phi \end{cases} \tag{17}$$

where the operator $\mathcal{L}(u_k, \delta u)$ is defined as follow:

$$\mathcal{L}(u_k, \delta u) = \int_{\phi_e} {}^T\nabla u_i : C_e : \nabla \delta u \, d\phi_e + E^*(0) \int_{\phi_v} {}^T\nabla u_i : C_0 : \nabla \delta u \, d\phi_v + E_i \int_{\phi_v} {}^T\nabla u_i : C_0 : \nabla \delta u \, d\phi_v \tag{18}$$

Since the nonlinear problem is represented as a set of linear problems, the principle of superposition applies to construct the localization tensors at every development order of ANM.

3.2. Localization tensors

Considering the scales coupling, the linear problem is first solved at every order of the ANM. The solution of the microscopic problem depends linearly on the imposed macroscopic strain. Therefore, the displacement u_k, can be decomposed into modes associated to different microscopic boundary conditions. Hence, in the 2D case, one can write:

$$u_k(X) = \{\tilde{u}_k^{11}(X), \tilde{u}_k^{22}(X), \frac{1}{2}[\tilde{u}_k^{12}(X) + \tilde{u}_k^{21}(X)]\} \begin{Bmatrix} \overline{\varepsilon}^{11} \\ \overline{\varepsilon}^{22} \\ 2\overline{\varepsilon}^{12} \end{Bmatrix} \quad \forall X \in \phi \tag{19}$$

where $\tilde{u}_k^{ij}$ are solutions at order k of the following problems:

$$\begin{cases} \mathcal{L}(\tilde{u}_k^{(ij)}, \delta u) = 0 & \forall X \in \phi \\ \tilde{u}_k^{(ij)+} - \tilde{u}_k^{(ij)-} = X^{(ij)+} - X^{(ij)-} & \forall X \in \partial\phi \end{cases} \tag{20}$$

with:

$$\begin{aligned} \tilde{u}_k^{(11)+} - \tilde{u}_k^{(11)-} &= \begin{bmatrix} 1 & 0 \\ 0 & 0 \end{bmatrix} (X^+ - X^-) \\ \tilde{u}_k^{(22)+} - \tilde{u}_k^{(22)-} &= \begin{bmatrix} 0 & 0 \\ 0 & 1 \end{bmatrix} (X^+ - X^-) \\ \tilde{u}_k^{(12)+} - \tilde{u}_k^{(12)-} &= \begin{bmatrix} 0 & 1 \\ 0 & 0 \end{bmatrix} (X^+ - X^-) \\ \tilde{u}_k^{(21)+} - \tilde{u}_k^{(21)-} &= \begin{bmatrix} 0 & 0 \\ 1 & 0 \end{bmatrix} (X^+ - X^-) \end{aligned} \tag{21}$$

The exponents (ij) indicate that the sought response is related to the component $\overline{\varepsilon}^{ij}$ of the macroscopic strain tensor. By denoting the tensor A_k by $\mathbb{A}_k = \{\tilde{u}_k^{11}, \tilde{u}_k^{22}, \frac{1}{2}(\tilde{u}_k^{12} + \tilde{u}_k^{21})\}$, the solution $u = u_0 + \sum_{i=1}^N a^i u_i$ can be written as follows:

$$u = \mathbb{A} : \overline{\varepsilon} \tag{22}$$

where $\mathbb{A} = \mathbb{A}_0 + \sum_{i=1}^N a^i \mathbb{A}_i$. $\mathbb{A}$ is a third-order tensor defined by $\mathcal{A}_{(ijp)} = \tilde{u}_{(i)}^{(jp)}$. The introduction of the Eq. (22) in the definition of the microscopic tensor ε, gives:

$$\varepsilon = \mathbb{A}_{,X} : \overline{\varepsilon} \tag{23}$$

where $\mathbb{A}_{,X} = \frac{1}{2}\left(\nabla\mathbb{A} + {}^T\nabla\mathbb{A}\right)$ is a fourth-order tensor identified as localization tensor.

3.3. Microscopic problem solving

3.3.1. Discretization by finite element method

The microscopic problem is solved by finite element analysis. After discretization, the microscopic problem can be written as follows:

$$\begin{cases} [K_0 + E(\lambda)K_v]u_0 = 0 & \forall X \in \phi \\ u_0^+ - u_0^- = X^+ - X^- & \forall X \in \partial\phi \end{cases} \tag{24}$$

By using power series expansion of Eq. (15) in Eq. (24), one can write the problem to be solved at each order of ANM as follows:

Order 1.

$$\begin{cases} [K_T]u_1 = -E_1 K_v u_0 & \forall X \in \phi \\ u_1^+ - u_1^- = 0 & \forall X \in \partial\phi \end{cases} \tag{25}$$

Order $k \geq 2$.

$$\begin{cases} [K_T]u_k = -\sum_{n=0}^{k-1} E_{k-n} K_v u_n & \forall X \in \phi \\ u_k^+ - u_k^- = 0 & \forall X \in \partial\phi \end{cases} \tag{26}$$

It should be noted that at each development order of ANM, there is only one equation but with two unknowns and a second equation is therefore needed. The definition of the path parameter a will provide this second equation at each order:

$$a = \frac{1}{S^2}\{(u(a) - u_0) \cdot u_1 + (\lambda(a) - \lambda_0) \cdot \lambda_1\} \tag{27}$$

By introducing the power series development in Eq. (15) into the definition of the parameter a in Eq. (27), one obtains a second equation at each order of ANM. The system of equations to be solved at each order can thus be written as follow:

Order 1.

$$\begin{cases} [K_T]u_1 = -E_1 K_v u_0 & \forall X \in \phi \\ u_1^2 + \lambda_1^2 = S^2 & \\ u_1^+ - u_1^- = 0 & \forall X \in \partial\phi \end{cases} \tag{28}$$

Order $k \geq 2$.

$$\begin{cases} [K_T]u_k = -\sum_{n=0}^{k-1} E_{k-n} K_v u_n & \forall X \in \phi \\ {}^T u_k u_1 + \lambda_k \lambda_1 = 0 & \\ u_k^+ - u_k^- = 0 & \forall X \in \partial\phi \end{cases} \tag{29}$$

3.3.2. Automatic differentiation

In the classical version of the ANM, the higher-order differentiation recurrence formula used to calculate the Taylor coefficients u_k, λ_k and E_k of u, λ and E are analytically determined. As discussed in [5], Automatic Differentiation (AD) offers an efficient technical solution for derivative computations. In Automatic Differentiation, any numerical model $b = f(a)$ is viewed as a sequence of elementary operations. The automatic derivation of f is performed by applying the chain rule to the sequence of h comprising f. Higher order AD relies in practice on operator overloading as the vehicle of attaching derivative computations to the elementary operations h provided by the programming language such as the arithmetic operators and the intrinsic functions. Let $f(a) = hox(a)$ be an analytical function. From a theoretical point of view, considering the Faà di Bruno recurrence formula written in terms of Bell polynomials [5]:

$$f_n = (hox)_n = \sum_{m=1}^{n} \frac{1}{n!} \frac{\partial^m h}{\partial x^m}(x_0) B_{n,m}(x^{(1)}, \ldots, x^{(n-m+1)}) \tag{30}$$

This is a short and effective way to present the Diamant interpretation of the ANM [5] where f_n could be split into two parts:

$$f_n = \{f_{1|x_1=1}\}x_n + \{f_{n|x_n=0}\} \tag{31}$$

On one hand, $\{f_{1|x_1=1}\}$ is the tangent linear derivative evaluated at $x_1 = 1$. On the other hand, the second term is the Taylor coefficient f_n evaluated at $x_n = 0$ to cancel the contribution of $\{f_{1|x_1=1}\}$. Applying the decomposition in Eq. (30) to E_k in the microscopic problems in Eqs. (28) and (29) yields:

Order 1.

$$\begin{cases} [K_T]u_1 = -\lambda_1\{E_{1|\lambda_1=1}\}K_v u_0 & \forall X \in \phi \\ u_1^2 + \lambda_1^2 = S^2 & \\ u_1^+ - u_1^- = 0 & \forall X \in \partial\phi \end{cases} \tag{32}$$

Order $k \geq 2$.

$$\begin{cases} [K_T]u_k = -\sum_{n=0}^{k-1}\lambda_{k-n}\{E_{1|\lambda_1=1}\}K_v u_n - \sum_{n=0}^{k-1}\{E_{k-n|\lambda_{k-n}=0}\}K_v u_n \\ \qquad \forall X \in \phi \\ {}^T u_k u_1 + \lambda_k\lambda_1 = 0 \\ u_k^+ - u_k^- = 0 \quad \forall X \in \partial\phi \end{cases} \tag{33}$$

The solutions of the microscopic problems at every order k can be written as follows:

Solution at order 1.

$$\begin{cases} \widehat{u}_1 = -\{E_{1|\lambda_1=1}\}K_T^{-1}K_v u_0 \\ \lambda_1 = \pm\dfrac{S}{\sqrt{1 + {}^T\widehat{u}_1\widehat{u}_1}} \\ u_1 = \lambda_1\widehat{u}_1 \end{cases} \tag{34}$$

Solution at order $k \geq 2$.

$$\begin{cases} \widehat{u}_k = -K_T^{-1}K_v(\{E_{1|\lambda_1=1}\}\sum_{n=1}^{k-1}\lambda_{k-n}u_n + \sum_{n=0}^{k-1}\{E_{k-n|\lambda_{k-n}=0}\}u_n) \\ \lambda_k = -\lambda_1\dfrac{{}^T u_1\widehat{u}_k}{S^2} \\ u_k = \dfrac{\lambda_k}{\lambda_1}u_1 + \widehat{u}_k \end{cases} \tag{35}$$

With this approach, once the frequency dependent Young's modulus is defined, the DIAMANT method [5] provides automatically the Taylor Series coefficients $\{E_{1|\lambda_1=1}\}$ and $\{E_{k-n|\lambda_{k-n}=0}\}$ at each step of the solution.

3.3.3. Continuation procedure

Solutions of the presented algorithm are accurate only in the vicinity of the starting solution (u^i, λ^i) due to the convergence radius of series. In fact, if the parameter a is larger than the convergence radius, the solution will not be accurate. Nevertheless, a very small value of the parameter a compared to the convergence radius will increase the number of needed iterations and CPU time. As usual in the ANM, the last term of the series is used to estimate the convergence radius:

$$a_{max} = (\hat{\delta}\frac{\|u_1\|}{\|u_N\|})^{\frac{1}{N-1}} \tag{36}$$

where $\hat{\delta}$ is a small parameter to be chosen. An optimal value of the truncated order of the series is $N = 20$ [39].

3.4. Homogenization tensor

By substituting the relation in Eq. (23) into Eq. (7), the microscopic stress–strain law can be written as follows:

$$\sigma = C^{(r)} : \mathbb{A}_{,X} : \overline{\varepsilon} \tag{37}$$

Substituting the relation in Eq. **??** into the average relation of Hill (8), one can write:

$$\overline{\sigma} = \langle C^{(r)} : \mathbb{A}_{,X}\rangle : \overline{\varepsilon} = \frac{1}{|\phi|}\int_\phi C^{(r)} : \mathbb{A}_{,X} : \overline{\varepsilon}\, d\phi \tag{38}$$

Considering the macroscopic stress–strain law (3), the fourth-order tensor $(\overline{C})$ of the behaviour of the macroscopic structure is identified as follows:

$$\overline{C} = \langle C^{(r)} : \mathbb{A}_{,X}\rangle = \frac{1}{|\phi|}\int_\phi C^{(r)} : \mathbb{A}_{,X}\, d\phi \tag{39}$$

Finally, the macroscopic behaviour is computed from the microscopic one, and thus the macroscopic problem can be discretized and solved by the finite element procedure. It should be noted that only the free vibration is studied here. Based on the presented methodological approach, the free vibration problem of the considered heterogeneous structure can be investigated by discretizing the problem in Eq. (2) and numerically solving the following linear complex eigenvalue problem at macroscale:

$$([\overline{K}] - \lambda[\overline{M}])\{\overline{U}\} = 0 \tag{40}$$

where $[\overline{K}]$ is a complex macroscopic stiffness matrix and $[\overline{M}]$ denotes the macroscopic mass matrix. λ represents the eigenvalue. The eigenvalue problem (40) leads to complex eigenvalues (λ_n) from which the damping properties of the structure are calculated in the following form:

$$\begin{cases} \Omega_n = \sqrt{\Re(\lambda_n)} \\ \eta_n = \dfrac{\Im(\lambda_n)}{\Re(\lambda_n)} \end{cases} \tag{41}$$

where $\Re(\lambda_n)$ and $\Im(\lambda_n)$ are respectively the real and imaginary parts of the nth eigenvalue λ_n.

4. Verification and validation tests

Verification and validation (V&V) of the developed approach and model are critical to build credibility and confidence in model predictions for engineering design analysis. V&V are performed on two typical examples: (1) a visco-elastically damped composite structure and (2) a sandwich beam with a heterogeneous visco-elastic core. To show the flexibility of the approach, heterogeneous composite structures with visco-elastic material in the matrix and elastic material for the inclusions and vice versa as well several frequency dependence laws governing the Young's modulus evolution are considered.

In the two analysed examples, the reference solution (one scale model) is discretized using a plane stress six-node triangular finite element model. In the multi-level approach, the RVE of the microscale model is discretized using a three-node triangular element while at the macroscale a nine node quadrangular element is used. A truncation order of $N = 20$ is considered in the ANM development and the parameter $\hat{\delta}$ intervening in the estimation a_{max} of the convergence radius is chosen equal to 10^{-6}. The results of the proposed approach are in very good agreement when compared to the reference one. In addition, the results show excellent agreement when compared to those in [23] for the sandwich use-case.

4.1. Application to vibration analysis of heterogeneous structures

4.1.1. Case of constant visco-elastic modulus

The Young's modulus of visco-elastic phases is approximated by a constant complex model:

$$E_{ve}^*(\omega) = E_0(1 + i\eta_{ve}) \tag{42}$$

The real Young's modulus, E_0, is related to the delayed elasticity and η_{ve} is the loss factor of visco-elastic material. Material and geometrical properties of the considered heterogeneous cantilever beam are reported in Table 1.

The inclusions are circular and represent 28% of the volume of the structure. Two cases are considered for the loss factors of the visco-elastic material $\eta_{ve} \in \{0.6, 1.5\}$. For the full model (reference solution), the structure is discretized in Abaqus Finite Element Solver using 100870 CPS6M elements involving 1217804 degrees of freedom (dofs). On the counterpart, only 770 elements involving 824 dofs at the microscale and 500 elements involving 4242 dofs at the macroscale are needed for the multi-level FE^2.

Table 1
Material and geometrical properties of the heterogeneous cantilever beam.

Elastic material	Young modulus	$E_e = 10^9$Pa
	Poisson's ratio	$\nu_e = 0.45$
	Density	$\rho_e = 1550$ kg/m^3
Viscoelastic material	Young modulus	$E_{ve} = 1794 \times 10^4$ Pa
	Poisson's ratio	$\nu_{ve} = 0.3$
	Density	$\rho_{ve} = 968.1$ kg/m^3
Beam dimensions	Length	$L = 0.2$ m
	Thickness	$h = 0.04$ m

The first validation (Table 2) concerns an elastic matrix with a visco-elastic inclusions. The second validation, reported on (Table 3), is a structure with visco-elastic matrix and an elastic inclusions.

We report the first four global resonant frequencies and modal loss factors of the analysed cantilever beam. One can see that the results of the presented approach are in good agreement with the full discretized model solved in Abaqus as well as those available in the literature with relative errors less than 1% for the resonant frequencies. Significant to be reported that only one iteration and 64 seconds are needed to compute the sixteen modal properties using the proposed approach when 33 hours are needed to perform the same computation using a commercial software like Abaqus.

4.1.2. Frequency dependent visco-elastic modulus

The goal of this section is to show the validity of the new approach regardless of the frequency dependence law governing the evolution of the Young's modulus of the visco-elastic material. The shear modulus of the visco-elastic Polyvinyl butyral Polymer (PVB) may be approximated at 20 °C by a fractional derivative model:

$$G_{ve}(\omega) = G_\infty + (G_0 - G_\infty)[1 + (i\omega\tau)^{1-\alpha}]^{-\beta} \tag{43}$$

where $G_0 = 479 \times 10^3$ Pa, $G_\infty = 2.35 \times 10^8$ Pa, $\tau = 0.3979$, $\alpha = 0.46$, $\beta = 0.1946$. Geometrical and material characteristics of the considered heterogeneous beam are given in Table 5. Inclusions are circular and represents 60% of the volume of the structure. Clamped beam boundary conditions are considered.

For the computation of the full model, 399716 CPS6M elements leading to 2401858 dofs and roughly about 45 hours computing time are needed. On the counterpart for the proposed method, only 2722 elements leading to 2844 dofs are needed for the microscopic problem whereas 3200 elements leading to 26332 dofs are needed for solving of the macroscopic problem. The calculation of the eight modal properties need approximately 77 minutes of computation time.

Resonant frequencies and modal loss factors, computed using the presented approach, are compared to those of the full model as presented in Table 4. One can see through these results that, the first four damping properties are in good agreement. The efficiency of the proposed approach compared to the fully resolved model, is demonstrated. In this specific case, the ANM procedure needs seven iteration per mode.

4.2. Application for the vibration analysis of a sandwich beam

The goal of this subsection is to assess the efficiency of the proposed method in computation of modal properties of visco-elastic sandwich structures with a heterogeneous visco-elastic core. In order to improve the damping properties of the sandwich beam with visco-elastic core, another visco-elastic material with the high damping properties can be added as inclusions in the core, see Fig. 3.

The faces are in glass, and the core is heterogeneous with PVB matrix and 3M ISD112 inclusions. The PVB is considered at 20 °C

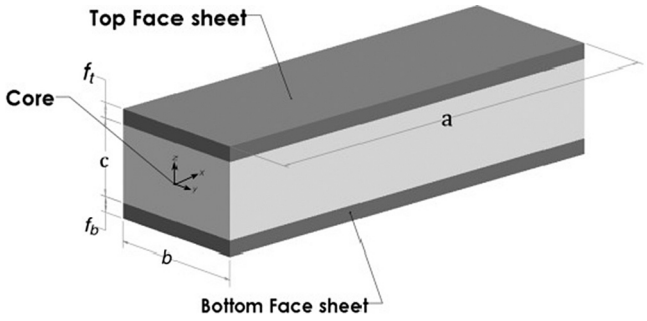

Fig. 3. Schematic representation of the sandwich beam with heterogeneous core. *Source:* Image taken from [40].

and its shear modulus is given by Eq. (43). The 3M ISD112 is also considered at 20 °C and its Young's modulus is given by [6]:

$$G^*_{ve}(\omega) = G_0(1 + \sum_{j=1}^{3} \frac{\Delta_j \omega}{\omega - i\Omega_j}) \tag{44}$$

where the parameters G_0 and (Δ_j, Ω_j) are given in Table 8. Geometrical and material characteristics of considered Glass/PVB-3M ISD112/Glass sandwich beam are given in Table 9. Inclusions are horizontal elliptic and represents 40% of the volume of the structure. Clamped beam boundary conditions are considered.

The predicted resonant frequencies and modal loss factors are compared in Table 6. The results obtained with both methods are in good agreement. The presented approach is thus efficient to compute the damping properties of the visco-elastic sandwich beam with heterogeneous core in case of the frequency dependent modulus (Table 7).

5. Application: Design of visco-elastic sandwich structures with high damping properties

The aim of this section is to assess the ability of the proposed methodological approach to optimize the damping properties of the visco-elastic sandwich structures. To achieve this goal, let us consider a Glass/PVB/Glass sandwich beam under the clamped–clamped boundary conditions. The material and geometrical properties of the considered beam are given in Table 9. The shear modulus of PVB at 20 °C is approximated by the fractional derivative model Eq. (43). In order to improve the damping properties of the beam, 3M ISD112 inclusions are added in the PVB core. The shear modulus of the 3M ISD112 at 20 °C is given by the ADF model in Eq. (44). The influence of the volume fraction and the morphology of the 3M ISD112 inclusions on the damping properties of the beam, are assessed based on the proposed approach.

5.1. Volume fraction effect

To assess the influence of the volume fraction of inclusions on damping properties, we vary the volume fraction of 3M ISD112 inclusions from 0% (corresponding to Glass/PVB/Glass beam) to 100% (corresponding to a Glass/3M ISD112/Glass beam). The considered inclusions are horizontal elliptic. Evolution of the three first resonant frequencies and modal loss factors according to the evolution of the volume fraction of inclusions are plotted in Figs. 4 and 5. One can note from Fig. 5 that the modal loss factors increase when the volume fraction of 3M ISD112 increases. This occurs since the 3M ISD112 is softer than PVB at 20 °C. Indeed, in the sandwich structures with a visco-elastic core, the damping is mainly due to the shear deformation in the visco-elastic core especially when the faces are stiffer than the core [6]. Nevertheless, the resonant frequencies decrease when the volume fraction of 3M ISD112 increases as showed by Fig. 4. Thus, increasing of the volume fraction of 3M ISD112 leads to loss of rigidity in the whole structure.

Table 2
Comparative results for the resonant frequencies (Ω) and the modal loss factors (η) obtained by the presented approach and the fully resolved model (FRM) in the case of the cantilever beam where the matrix is elastic and the inclusions are viscoelastic.

η_{ve}	Modes	Presented approach				FRM		Attipou et al. [23]	
		Ω (Hz)	%ER	η/η_{ve}	%ER	Ω (Hz)	η/η_{ve}	Ω (Hz)	η/η_{ve}
0.6	1	96.45	0.10	0.030	3.44	96.54	0.029	97.00	0.029
	2	498.34	0.30	0.041	0.00	496.86	0.041	502.62	0.0385
	3	1154.68	0.44	0.047	−4.08	1149.67	0.049	1166.68	0.0442
	4	1878.80	0.34	0.052	−5.45	1871.28	0.055	1901.02	0.0486
1.5	1	96.51	0.00	0.030	7.14	96.51	0.028	–	–
	2	498.91	0.22	0.041	2.50	497.79	0.040	–	–
	3	1156.25	0.72	0.047	−2.08	1148.04	0.048	–	–
	4	1881.62	0.26	0.052	−1.89	1876.82	0.053	–	–

Table 3
Comparative results for the resonant frequencies (Ω) and the modal loss factors (η) obtained by the presented approach and the fully resolved model (FRM) in the case of the cantilever beam where the matrix is viscoelastic and the inclusions are elastic.

η_{ve}	Modes	Presented approach				FRM	
		Ω (Hz)	%ER	η	%ER	Ω (Hz)	η
0.6	1	25.39	0.63	0.586	0	25.23	0.586
	2	135.56	0.54	0.587	0	134.83	0.587
	3	321.00	0.46	0.588	0	319.52	0.588
	4	531.08	0.40	0.589	0	528.94	0.589
1.5	1	25.77	0.62	1.421	−0.07	25.61	1.422
	2	137.48	0.54	1.427	0	136.74	1.427
	3	325.29	0.46	1.431	0	323.81	1.431
	4	537.83	0.39	1.434	0.07	535.73	1.433

Table 4
Comparative results for the resonant frequencies (Ω) and the modal loss factors (η) obtained by the presented approach and the fully resolved model (FRM) in the case of the C–C beam with PVB at 20 °C.

Matrix elastic and Inclusions viscoelastic						
Modes	Presented approach			FRM		
	Ω (Hz)	%ER	η	%ER	Ω (Hz)	η
1	551.62	0.02	0.0324	0.00	551.72	0.0324
2	1262.39	0.25	0.0361	0.27	1265.58	0.0362
3	2111.84	0.45	0.0370	0.27	2121.30	0.0369
4	3028.24	–	0.0375	–	–	–
Matrix viscoelastic and Inclusions elastic						
Modes	Presented approach			FRM		
	Ω (Hz)	%ER	η	%ER	Ω (Hz)	η
1	401.34	1.96	0.136	2.16	393.63	0.139
2	1000.08	1.83	0.115	1.71	982.14	0.117
3	1753.67	1.44	0.105	6.25	1728.76	0.112
4	2595.14	–	0.098	–	–	–

Table 5
Geometrical and material characteristics of the considered clamped–clamped heterogeneous beam containing PVB at 20 °C.

Elastic material	Young modulus	$E_e = 16.015 \times 10^9$ Pa
	Poisson's ratio	$\nu_e = 0.44$
	Density	$\rho_e = 490$ kg/m^3
Viscoelastic material	Shear modulus	$G_0 = 479 \times 10^3$ Pa
	Poisson's ratio	$\nu_{ve} = 0.4$
	Density	$\rho_{ve} = 999$ kg/m^3
Beam dimensions	Length	$L = 0.4$ m
	Thickness	$h = 0.05$ m

5.2. Influence of the shape of inclusions

In the considered heterogeneous structures, the fibre inclusions can have three morphologies: horizontal elliptic, circular and vertical elliptic. In this section we assess the influence of every morphology on the damping properties of sandwich beams with a visco-elastic core.

Table 6
Resonant frequencies (Ω) and modal loss factor (η) of the considered Glass/PVB-3M ISD112/Glass sandwich beam under clamped–clamped boundary conditions.

Modes	Presented approach				ABAQUS	
	Ω (Hz)	%ER	η	%ER	Ω (Hz)	η
1	93.75	−1.42	0.109	0.00	95.10	0.109
2	231.94	−1.07	0.0760	−1.55	234.44	0.0772
3	428.64	−0.54	0.0620	−1.81	430.96	0.0609
4	681.79	−0.25	0.0460	−1.50	683.48	0.0467

Table 7
Comparative results for the resonant frequencies (Ω) and the modal loss factors (η) obtained by the presented approach and the fully resolved model (FRM) in the case of the C–C beam with PVB at 20 °C.

Matrix elastic and Inclusions viscoelastic						
Modes	Presented approach				FRM	
	Ω (Hz)	%ER	η	%ER	Ω (Hz)	η
1	551.62	0.02	0.0324	0.00	551.72	0.0324
2	1262.39	0.25	0.0361	0.27	1265.58	0.0362
3	2111.84	0.45	0.0370	0.27	2121.30	0.0369
4	3028.24	–	0.0375	–	–	–
Matrix viscoelastic and Inclusions elastic						
Modes	Presented approch				FRM	
	Ω (Hz)	%ER	η	%ER	Ω (Hz)	η
1	401.34	1.96	0.136	2.16	393.63	0.139
2	1000.08	1.83	0.115	1.71	982.14	0.117
3	1753.67	1.44	0.105	6.25	1728.76	0.112
4	2595.14	–	0.098	–	–	–

Table 8
Fit-parameters of the 3M ISD112 at 20 °C.

j	G_0 (Pa)	Δ_j	Ω_j (rad/s)
1		2.8164	31.1176
2	0.0511×10^6	13.1162	446.4542
3		45.4655	5502.5318

Table 9
Material and geometrical properties of the considered Glass/PVB-3M ISD112/Glass sandwich beam.

Elastic faces	Young modulus	$E_f = 64.5 \times 10^9$ Pa
	Poisson's ratio	$\nu_f = 0.22$
	Density	$\rho_f = 2737$ kg/m^3
	Thickness	$h_f = 9 \times 10^{-3}$ m
Viscoelastic core	Poisson's ratio of the matrix	$\nu_{0m} = 0.4$
	Density of the matrix	$\rho_{0m} = 999$ kg/m^3
	Poisson's ratio of inclusions	$\nu_{0i} = 0.5$
	Density of inclusions	$\rho_{0i} = 1600$ kg/m^3
	Thickness	$h_c = 4 \times 10^{-3}$ m
Whole structure dimensions	Length	$L = 800 \times 10^{-3}$ m
	Thickness	$h = 22 \times 10^{-3}$ m

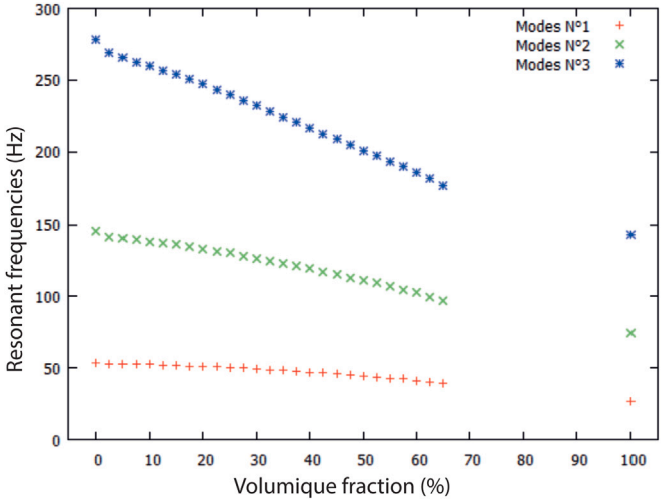

Fig. 4. Evolution of three first resonant frequencies (Ω) according to the evolution of volume fractions of inclusions.

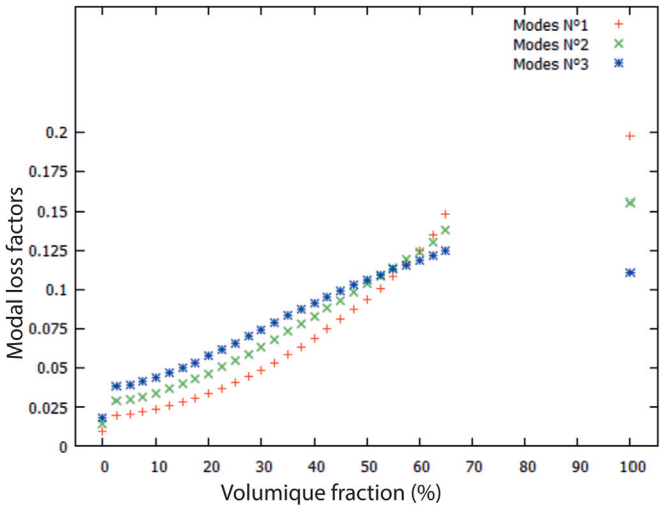

Fig. 5. Evolution of three first modal loss (η) factors vs of volume fraction of the inclusions.

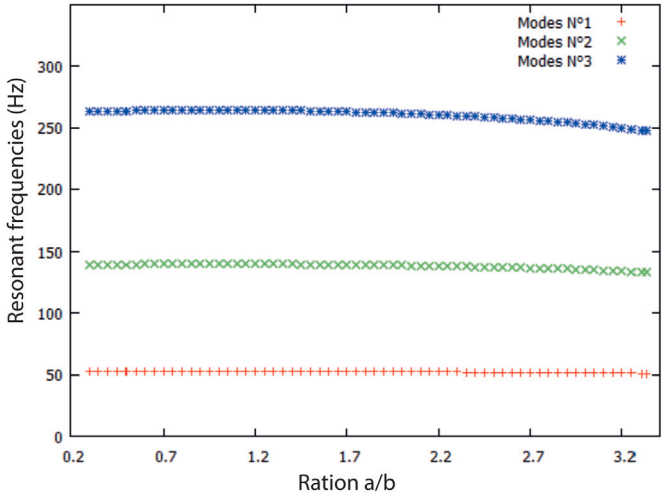

Fig. 6. Evolution of the three first resonant frequencies (Ω) according to the morphology of the inclusions.

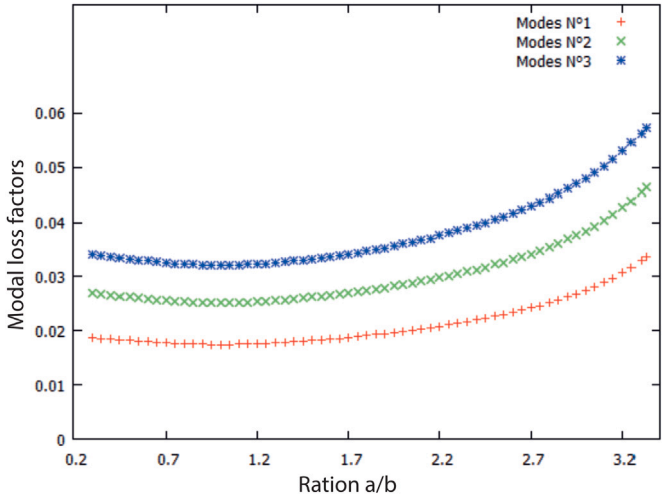

Fig. 7. Evolution of the three first modal loss factors (η) according to the morphology of the inclusions.

For this purpose, the multi-scale finite element approach developed previously is used to compute the damping properties of the considered sandwich beam according to the evolution of the ratio a_e/b_e. a_e and b_e are the principal axis of the ellipse that define the morphology of the inclusion. The inclusions are horizontal for $a_e/b_e > 1$, circular for $a_e/b_e = 1$ and vertical elliptic for $a_e/b_e < 1$. The volume fraction of the fibre inclusions is fixed at 20%. For a fixed volume fraction of inclusions, we assess the influence of their morphology on damping properties. The evolution of the three first resonant frequencies and the modal loss factors according to the ratio a_e/b_e are plotted on Figs. 6 and 7. The ratio a_e/b_e has no significant influence on the resonant frequencies while the modal loss factors vary according to the ratio a_e/b_e as clearly demonstrated in Figs. 6 and 7. It should be noted that the lower modal loss factors correspond to circular ($a_e/b_e = 1$) fibre inclusions whereas the highest values of modal loss factors correspond to the highest value of the ratio a_e/b_e. This allows one to increase the damping effects based on the inclusions morphology.

6. Conclusion

A multi-scale finite element approach has been proposed to compute the damping properties of visco-elastically damped composite structures. The non linear vibration problem is solved using the ANM combined to the automatic differentiation method and tool. The analysed use-cases demonstrate the flexibility, the accuracy and the efficiency of the proposed numerical approach. The flexibility results from the use of automatic differentiation which allows for analysing different structural configurations regardless the used material frequency dependent laws. As regards the efficiency, the proposed approach allows for analysing constant and frequency dependent Young's modulus with a massive reduction of CPU time.

Declaration of competing interest

The authors declare that they have no known competing financial interests or personal relationships that could have appeared to influence the work reported in this paper.

Acknowledgements

The authors from Luxembourg Institute of Science and Technology acknowledge the financial support of Fonds National de la Recherche, Luxembourg (FNR) through the Grant DeeMA: INTER/MERA20/15011099. The authors from the University of Lorraine acknowledge the financial support from French State program "Investment in the future" operated by the Agence Nationale de La Recherche (ANR)-LabEx DAMAS.

References

[1] F. Mastroddi, F. Martarelli, M. Eugeni, C. Riso, Time-and frequency-domain linear viscoelastic modeling of highly damped aerospace structures, Mech. Syst. Signal Process. 122 (2019) 42–55.
[2] Nitin Choudhary, Davinder Kaur, Vibration damping materials and their applications in nano/micro-electro-mechanical systems: a review, J. Nanosci. Nanotechnol. 15 (3) (2015) 1907–1924.
[3] E.M. Daya, M. Potier-Ferry, A numerical method for nonlinear eigenvalue problems application to vibrations of viscoelastic structures, Comput. Struct. 79 (5) (2001) 533–541.
[4] Lt. Duigou, El Mostafa Daya, Michel Potier-Ferry, Iterative algorithms for nonlinear eigenvalue problems. Application to vibrations of viscoelastic shells, Comput. Methods Appl. Mech. Eng. 192 (11–12) (2003) 1323–1335.
[5] Y. Koutsawa, I. Charpentier, E.M. Daya, M. Cherkaoui, A generic approach for the solution of nonlinear residual equations. Part I : The Diamant toolbox, Comput. Methods Appl. Mech. Eng. 198(3-4) (2008) 572–577.
[6] Massamaesso Bilasse, Isabelle Charpentier, El Mostafa Daya, Yao Koutsawa, A generic approach for the solution of nonlinear residual equations. Part II: Homotopy and complex nonlinear eigenvalue method, Comput. Methods Appl. Mech. Eng. 198 (49–52) (2009) 3999–4004.
[7] F. Abdoun, L. Azrar, E.M. Daya, M. Potier-Ferryc, Forced harmonic response of viscoelastic structures by an asymptotic numerical method, Comput. Struct. 87 (11–20) (2009) 91–100.
[8] Yao Koutsawa, Wiyao Leleng Azoti, Salim Belouettar, Rodolphe Martin, Evgeny Barkanov, Loss behavior of viscoelastic sandwich structures: A statistical-continuum multi-scale approach, Compos. Struct. 94 (4) (2012) 1391–1397.
[9] Marco Montemurro, Yao Koutsawa, Salim Belouettar, Angela Vincenti, Paolo Vannucci, Design of damping properties of hybrid laminates through a global optimisation strategy, Compos. Struct. 94 (11) (2012) 3309–3320.
[10] Heng Hu, Salim Belouettar, Michel Potier-Ferry, et al., Review and assessment of various theories for modeling sandwich composites, Compos. Struct. 84 (3) (2008) 282–292.
[11] Houssein Nasser, El-Hassania Kiefer-Kamal, Heng Hu, Salim Belouettar, Evegny Barkanov, Active vibration damping of composite structures using a nonlinear fuzzy controller, Compos. Struct. 94 (4) (2012) 1385–1390.
[12] QZ He, Heng Hu, Salim Belouettar, G Guinta, Kun Yu, Yin Liu, Fabio Biscani, Erasmo Carrera, Michel Potier-Ferry, Multi-scale modelling of sandwich structures using hierarchical kinematics, Compos. Struct. 93 (9) (2011) 2375–2383.
[13] Houssein Nasser, El-Hassania Kiefer-Kamal, Heng Hu, Salim Belouettar, Evegny Barkanov, Active vibration damping of composite structures using a nonlinear fuzzy controller, Compos. Struct. 94 (4) (2012) 1385–1390.
[14] Hakim Boudaoud, Salim Belouettar, El Mostafa Daya, Michel Potier-Ferry, A shell finite element for active-passive vibration control of composite structures with piezoelectric and viscoelastic layers, Mech. Adv. Mater. Struct. 15 (3–4) (2008) 208–219.
[15] Komlan Akoussan, Hakim Boudaoud, El-Mostafa Daya, Erasmo Carrera, Vibration modeling of multilayer composite structures with viscoelastic layers, Mech. Adv. Mater. Struct. 22 (1–2) (2015) 136–149.
[16] L. Azrar, S. Belouettar, J. Wauer, Nonlinear vibration analysis of actively loaded sandwich piezoelectric beams with geometric imperfections, Comput. Struct. 86 (23–24) (2008) 2182–2191.
[17] Heng Hu, Salim Belouettar, El Mostafa Daya, Michel Potier-Ferry, Evaluation of kinematic formulations for viscoelastically damped sandwich beam modeling, J. Sandw. Struct. Mater. 8 (6) (2006) 477–495.
[18] Christian Miehe, Serdar Göktepe, A micro–macro approach to rubber-like materials. Part II: The micro-sphere model of finite rubber viscoelasticity, J. Mech. Phys. Solids 53 (10) (2005) 2231–2258.
[19] WL Azoti, N Bonfoh, Y Koutsawa, S Belouettar, P Lipinski, Influence of auxeticity of reinforcements on the overall properties of viscoelastic composite materials, Mech. Mater. 61 (2013) 28–38.
[20] M. El Hachemi, Y. Koutsawa, H. Nasser, G. Giunta, A. Daouadji, E.M. Daya, S. Belouettar, An intuitive computational multi-scale methodology and tool for the dynamic modelling of viscoelastic composites and structures, Compos. Struct. 144 (2016) 131–137, http://dx.doi.org/10.1016/j.compstruct.2016.02.032.
[21] Adjovi Tchalla, Salim Belouettar, Ahmed Makradi, Hamid Zahrouni, An ABAQUS toolbox for multiscale finite element computation, Compos. Part B. Eng. 52 (2013) 323–333.
[22] F. Feyel, J.-L. Chaboche, FE^2 Multiscale approach for modelling the elastovisco-plastic behaviour of long fiber SiC/Ti composite materials, Comput. Methods Appl. Mech. Eng. 183 (2000) 309–330.
[23] Kodjo Attipou, Saeid Nezamabadi, El Mostafa Daya, Hamid Zahrouni, A multiscale approach for the vibration analysis of heterogeneous materials: Application to passive damping, J. Sound Vib. 332 (4) (2013) 725–739.
[24] Rui Xu, Celine Bouby, Hamid Zahrouni, Tarak Ben Zineb, Heng Hu, Michel Potier-Ferry, 3D Modeling of shape memory alloy fiber reinforced composites by multiscale finite element method, Compos. Struct. 200 (2018) 408–419, http://dx.doi.org/10.1016/j.compstruct.2018.05.108.
[25] Wei Huang, Rui Xu, Jie Yang, Qun Huang, Heng Hu, Data-driven multiscale simulation of FRP based on material twins, Compos. Struct. 256 (2021) 113013.
[26] Rui Xu, Jie Yang, Wei Yan, Qun Huang, Gaetano Giunta, Salim Belouettar, Hamid Zahrouni, Tarak Ben Zineb, Heng Hu, Data-driven multiscale finite element method: From concurrence to separation, Comput. Methods Appl. Mech. Eng. 363 (2020) 112893.
[27] Jie Yang, Rui Xu, Heng Hu, Qun Huang, Wei Huang, Structural-Genome-Driven Computing for composite structures, Compos. Struct. 215 (2019) 446–453.
[28] E.M. Daya, M. Potier-Ferry, A numerical method for nonlinear eigenvalue problems application to vibrations of viscoelastic structures, Comput. Struct. 79 (5) (2001) 533–541.
[29] Komlan Akoussan, Hakim Boudaoud, El Mostafa Daya, Yao Koutsawa, Erasmo Carrera, Numerical method for nonlinear complex eigenvalues problems depending on two parameters: Application to three-layered viscoelastic composite structures, Mech. Adv. Mater. Struct. 25 (15–16) (2018) 1361–1373.
[30] Fermin Otero, Sergio Oller, Xavier Martinez, Multiscale computational homogenization: review and proposal of a new enhanced-first-order method, Arch. Comput. Methods Eng. 25 (2) (2018) 479–505.
[31] R.K. Patel, B. Bhattacharya, S. Basu, A finite element based investigation on obtaining high material damping over a large frequency range in viscoelastic composites, J. Sound Vib. 303 (2007) 753–766.
[32] M. Koishi, M. Shiratori, T. Miyoshi, K. Kabe, Homogenization method for dynamic viscoelastic analysis of composite materials, JSME Int. J. SeriesA 40 (1997) 306–312.
[33] Y.M. Yi, S.H. Park, S.K. Youn, Design of microstructures of viscoelastic composites for optimal damping characteristics, Int. J. Solids Struct. 37 (2000) 4791–4810.
[34] R. Hill, Elastic properties of reinforced solids: some theoretical principles, J. Mech. Phys. Solids 11 (1963) 357–372..
[35] V. Kouznetsova, W.A.M. Brekelmans, F.P.T. Baaijens, An approach to micro-macro modeling of heterogeneous materials, Comput. Mech. 27 (2001) 37–48.
[36] J Menčík, G Rauchs, S Belouettar, J Bardon, A Riche, Modeling of response of viscoelastic materials to harmonic loading, in: Proceedings of Int. Conf. Engineering Mechanics 2004. Svratka, May 10, vol. 13, 2004, pp. 187–188.
[37] Yao Koutsawa, Salim Belouettar, Ahmed Makradi, Sonnou Tiem, Generalization of the micromechanics multi-coating approach to coupled fields composite materials with eigenfields: effective properties, Mech. Res. Commun. 38 (1) (2011) 45–51.
[38] L. Azrar, B. Cochelin, N. Damil, M. Potier-Ferry, An asymptotic-numerical method to compute the postbuckling behaviour of elastic plates and shells, Int. J. Numer. Methods Eng. 36 (8) (1993) 1251–1277.
[39] B. Cochelin, A path-following technique via an asymptotic-numerical method, Comput. Struct. 53(5) (1994) 1181–1192.
[40] Himanshu Sharma, Ranjan Ganguli, Optimization of a higher-order sandwich composite beam under uncertainties, Compos. Struct. 269 (2021) 114003.